

Membrane-type photonic-crystal microlasers for the integration of electronic and photonic ICs

J. Van Campenhout, P. Bienstman and R. Baets

Ghent University - IMEC, Dept. of Information Technology,
Sint-Pietersnieuwstraat 41, 9000 Gent, Belgium, Joris.VanCampenhout@intec.UGent.be

We propose two different approaches to achieve electrically pumped lasing in photonic-crystal based membrane-type devices. The first approach concerns a band-edge laser in an optically thick gold-clad photonic-crystal membrane. The second approach consists of a gold-clad ridge waveguide terminated with DBR-mirrors that is evanescently coupled to a passive waveguide. For both devices, a two-dimensional numerical analysis was performed, including gold absorption losses.

Introduction

In the last couple of years, several groups have reported lasing in membrane-type micron-sized photonic-crystal (PhC) cavities, both for defect-based cavities as for defect-free cavities (band-edge effect). These microlasers offer a great potential as microsources for the integration of electronic and photonic ICs. However, until now, only optically pumped devices have been demonstrated [1]. For practical applications, electrically pumped devices are essential. So there is a need for electrical contacting schemes for these microcavities, without giving up too much of their optical confinement quality. In this paper, we propose two different approaches to achieve electrically pumped lasing in membrane-type micron-sized devices. Both devices have different cavity types as well as different contacting schemes. The first approach concerns a surface-emitting band-edge laser with a very simple electrical contacting scheme, namely metal contacts both on top and bottom of the membrane. The second device concerns an ultrashort ridge waveguide with DBR mirrors on both side and a metal contact on top, and one on the side of the ridge waveguide. This device can be evanescently coupled to a passive waveguide underneath. Both devices have been analyzed numerically in a 2D cross section, by means of eigenmode expansion.

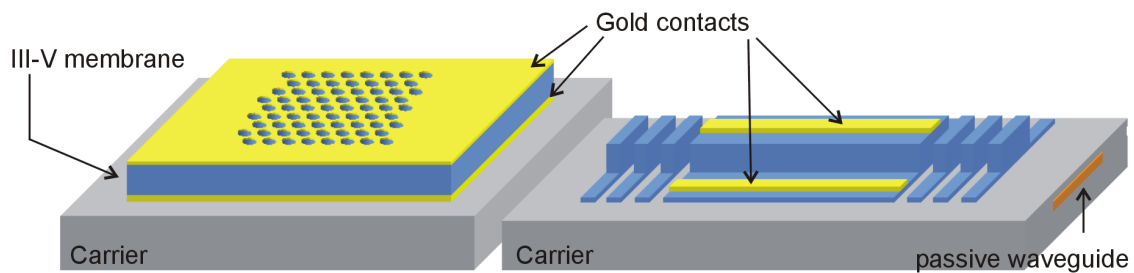


Figure 1: Layouts of two analyzed photonic-crystal based membrane-type laser devices

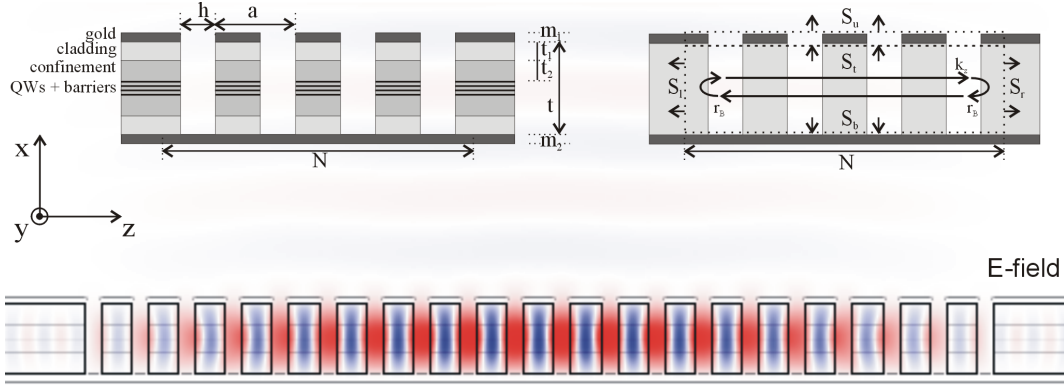


Figure 2: 2D Cross section of the surface-emitting band-edge microlaser

Surface-emitting band-edge microlaser

Consider the 2D structure in figure 2: a 1D photonic-crystal is etched in a gold-clad dielectric waveguide with a thickness t of about $1\mu\text{m}$. Gold was chosen as cladding metal due to the low absorption loss in the infrared region (around $1.5\mu\text{m}$) as compared to other - non-noble - metals. The dielectric waveguide consists of cladding layers ($n = 3.17$) and confinement layers ($n = 3.38$). Four 5-nm wide quantum wells (QW) are embedded centrally in the waveguide. Modal absorption losses (with transparent QW's) at an operating wavelength of $1.5\mu\text{m}$ were calculated as a function of total dielectric thickness t , both for TE- (electric field in the y -direction) as TM-polarization. For each thickness t , t_1 and t_2 have been chosen to yield the lowest modal absorption loss for the fundamental TE_0 -mode. The waveguide structure is monomode for $t < 0.45\mu\text{m}$. However, in this range, TE_0 absorption losses are too high to use the waveguide in a laser resonator. For $t > 0.45\mu\text{m}$, the waveguide becomes multimode and the absorption loss of modes far above cut-off decreases almost exponentially as a function of t , as progressively less of the field penetrates into the lossy gold layer. For TM, absorption losses are more than one order of magnitude higher than for the fundamental TE_0 -mode. For t around $1\mu\text{m}$, the propagation loss of the TE_0 -mode is around 15cm^{-1} . For the remainder of the text, we will assume TE-polarization and an operating wavelength around $1.5\mu\text{m}$.

Figure 3 shows the band diagram for a 1D gold-clad PhC with period $a = 665\text{nm}$, hole diameter $h = 210\text{nm}$, and gold thickness $m_{1,2} = 100\text{nm}$. The bands of the fundamental and the higher order modes are folded back due to the periodicity and band gaps are opened near the edges and the center of the Brillouin zone. At the same time, ministop-bands (MSB) are formed where two bands cross. Resonant modes with a high quality factor Q can be built up in a finite PhC for frequencies near the edges of the photonic bands where the group velocity $v_g = d\omega/dk$ is very low. A Bloch-mode propagating in an active PhC encounters a gain per unit length that is enhanced with a factor inversely proportional to v_g , as compared to a properly normalized bulk gain [2]. Moreover, the amplitude of the field reflection r_B of the Bloch-mode at the edges of the finite PhC-cavity increases when approaching a band edge. We have calculated laser resonances at Γ_1 and Γ_2 , which are both above the light line, so coupling to radiation modes is possible. However, due to symmetry mismatch, the TE_0 -mode is decoupled at Γ_1 , whereas it is leaky at Γ_2 . The resonance wavelength λ_r , quality factor Q and material threshold gain

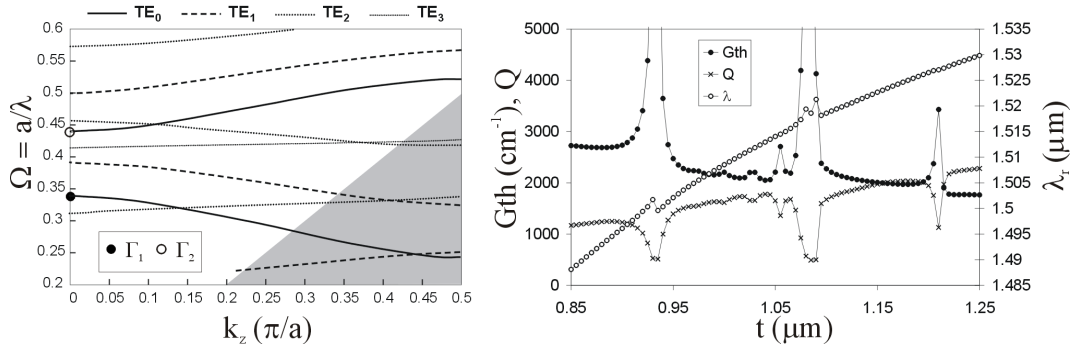


Figure 3: Band structure of the gold-clad PhC waveguide (left) and properties of the Γ_2 laser mode as a function of t (right).

G_{th} in the quantum wells of the Γ_2 laser mode are depicted in figure 3, as a function of t , for a cavity of 20 periods. There are three distinct peaks in the G_{th} - and Q -curves. For these t -values, the TE_0 -mode is coupled to a very lossy higher order mode and the quality of the resonance is poor. Apart from the peaks, the needed G_{th} -values are within range of gain levels in compressively strained QW's [3]. The surface emission efficiency (SEE) for $t = 1 \mu\text{m}$ is about 12.5 %, but can be increased by decreasing the thickness m_1 of the top gold layer. However, a higher SEE implies a higher threshold gain G_{th} . In order to have physical G_{th} -values, one might increase the cavity size, e.g. a 40-period cavity ($26.6 \mu\text{m}$) with $m_1 = 60 \text{ nm}$ has a SEE of 33.5 %, with a Q of 1860 and a G_{th} of 1900 cm^{-1} . For this device, metal losses contribute about 60 % of the cavity losses.

Ridge waveguide microlaser

Figure 4 shows a cross section of the ridge waveguide microlaser. A waveguide with length L , defined in a III-V membrane that is bonded on a SOI layer structure, is terminated with DBR mirrors. A gold layer is deposited on top. The III-V layer structure includes a cladding layer ($n = 3.17$) and a core layer ($n = 3.38$) whose thicknesses are optimized in order to reduce absorption losses. The total III-V thickness t is chosen to have the second higher order mode just below cut-off ($t = 600 \text{ nm}$). One QW is embedded centrally in the layer structure. A passive SOI waveguide can be placed underneath the cavity, with an intermediate SiO_2 -layer of thickness d .

High- Q Fabry-Pérot like resonances can be built up in this cavity, due to the high DBR reflectivity ($R > 96.9\%$) and the relatively low gold absorption loss. For an unloaded cavity with only one QW and a length $L = 14 \mu\text{m}$ is $G_{th} = 2700 \text{ cm}^{-1}$ and $Q = 3750$. This analysis doesn't include radiation losses in the y -direction, so the given Q -value is higher than the actual 3D Q -value. However, a 2D top down calculation of a $3 \mu\text{m}$ -wide, DBR-terminated ridge waveguide with a length $L = 14 \mu\text{m}$ yields resonances with quality factors up to 7500. So the main losses are included in a 2D cross sectional analysis.

The laser light can be coupled evanescently to an SOI-waveguide underneath the cavity. The amount of light coupled to the SOI-waveguide depends strongly on the cavity length L , and also on the bonding layer thickness d (see figure 4). The coupling length that can be deduced from the simulations is about $3 \mu\text{m}$ and agrees well with the coupling length L_c predicted by the directional coupler theory: $L_c = \frac{\pi}{\beta_0 - \beta_1} = 2.95 \mu\text{m}$,

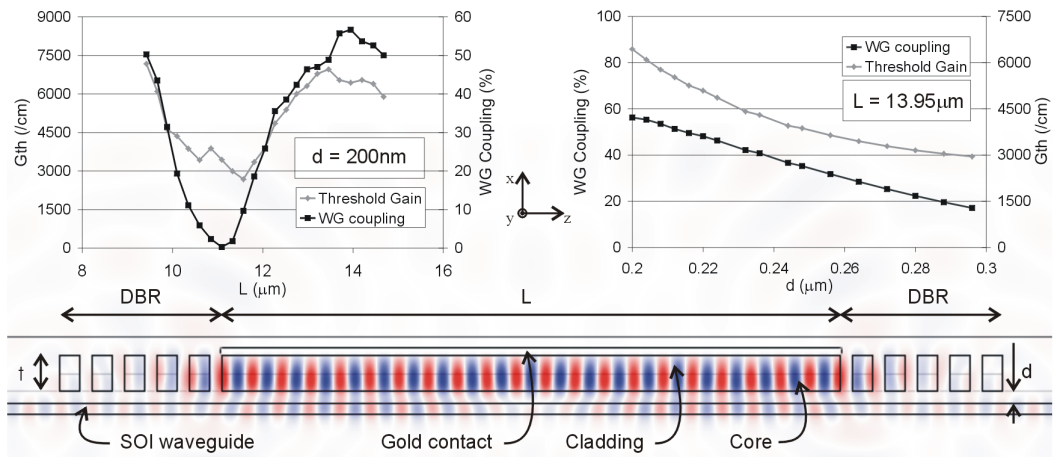


Figure 4: Cross section of the ridge waveguide microlaser

with β_0 and β_1 the propagation constants of the supermodes. For $d = 250\text{ nm}$ and $L = 13.95\ \mu\text{m}$, about 35% of the laser light is coupled to the SOI-waveguide and Q drops to 2500. The required material threshold gain G_{th} is 3850 cm^{-1} , for a single QW. Including 3 or 4 QWs in the III-V layer structure brings the required G_{th} -levels into physical reach.

Conclusion

We have numerically analyzed two different approaches to achieve electrically pumped lasing in membrane-type photonic crystal microlasers. A first device concerns a surface-emitting band-edge laser with gold contacts on both sides of the membrane. Quality factors Q are about 1860 combined with surface emission efficiencies above 30% for a cavity size of $26.6\ \mu\text{m}$. Metal losses contribute about 60% to the total cavity loss. A second approach concerns a ridge-waveguide based device terminated with DBR mirrors and a top and side gold contact. For an unloaded $14\ \mu\text{m}$ -long device the Q -factor is more than 3750. The laser light can be evanescently coupled to an SOI waveguide. This coupling can be tuned by changing the cavity length and the bonding layer thickness. For 35% extraction efficiency, the Q -factor drops to 2500. Depending on the specific application, a combination of these two approaches can result in an optimum laser cavity design.

Part of this work was performed in the context of the Belgian DWTC IAP-PHOTON project. J. Van Campenhout and P. Bienstman were supported by the Flemish Fund for Scientific Research (FWO-Vlaanderen) through a doctoral fellowship and postdoctoral fellowship, respectively.

References

- [1] Mouette, J. et al., "Very low threshold vertical emitting laser operation in InP graphite photonic crystal slab on silicon", *Electron. Lett.*, vol. 39, pp. 526–528, 2003.
- [2] Nojima, S., "Optical-gain enhancement in two-dimensional active photonic crystals", *J. Appl. Phys.*, vol. 90, pp. 545–551, 2001.
- [3] Ma, T.-A. and Li, Z.-M. and Makino, T. and Wartak, M. S., "Approximate Optical Gain Formulas for $1.55\text{-}\mu\text{m}$ strained quaternary quantum-well lasers", *IEEE J. Quant. Electron.*, vol. 31, pp. 29–34, 1995.